Analytical Investigation of Rupture Phenomena in Sheet Hydroforming Process by Hemispherical Punch

A. Naddaf Oskouei*, M. R. Elhami & I. Karami Fath
Department of Mechanical Engineering,
Faculty of Engineering, Imam Hossein University
Email: anadaf@ihu.ac.ir
*Corresponding author

Received: 11 December 2013, Revised: 13 May 2014, Accepted: 27 August 2014

Abstract: Rupture and wrinkling are two prevalent phenomena that happen in hydroforming process. Many efforts have been made to achieve the upper and lower bounds for the pressure related to rupture and wrinkling of sheet, respectively. The aim of this investigation is to improve the upper bound of fluid pressure in hydroforming process by hemispherical punch. In this article, analytical study of the upper bound of fluid pressure based on new assumption of Hill theory is presented. Next, governing equations of the process is derived, and numerical methods are used to solve these equations. In this process, the effect of material and geometric properties on the upper bound pressure is investigated. The results are compared with experimental and theoretical based on Tresca criterion. The study on the effect of geometry and material shows that increasing the sheet thickness raises the upper bound pressure. Moreover, the reduction of sheet to punch diameter ratio leads to increase of the upper bound pressure. On the other hand, decreasing the friction force as well as increasing the anisotropic coefficient both causes the rise of upper bound pressure. Finally, the increase of work hardening parameter leads to the rise of rupture point.

Keywords: Hydroforming Process, Rupture, Hill Theory, Material Anisotropy, Upper Bound Pressure, Lower Bound Pressure

Reference: Naddaf Oskouei, A., Elhami, M. R., and Karami Fath, I., "Analytical Investigation of Rupture Phenomena in Sheet Hydroforming Process by Hemispherical Punch", Int J of Advanced Design and Manufacturing Technology, Vol. 7/ No. 3, 2014, pp. 37-43.

Biographical notes: A. Naddaf Oskouei is currently Assistant Professor in Mechanical Engineering Department of the Imam Hossein University (IHU), Tehran, Iran. He received his PhD in Mechanical Engineering from Metz University, France. He has been working on modelling and numerical simulation, investigating various topics such as: contact modelling, elasto-plasticity and FEM. **M. Reza Elhami** received his PhD in Mechanical Engineering from Liverpool University, UK, in 1997. He is currently Assistant Professor at Mechanical Engineering Department of the Imam Hossein University (IHU), Tehran, Iran. He has been working on design and manufacturing of many industrial mechanisms in the field of control, dynamics and robotics. At present, his main research interest concern vibration analysis, advanced control strategies, intelligent mechanisms and advanced robotics. **I. Karami Fath** received his MSc from Imam Hossein University. He is currently a PhD student in Applied Mechanics of the Mechanical Engineering at Yasouj University, Iran. His current research interest is sheet metal forming.

1 INTRODUCTION

Sheet metal forming has wide application in industry where its products have various size and complexity. However, the price of tools used in sheet forming process is high, consequently increasing the cost of production. Hence, numerous studies in various fields of forming including hydroforming are being carried out to get perfect products at reasonable costs and minimum raw material consumption. One of the widely used products in industry is spherical shape products. Making this type of products, either by deep drawing or other methods, involves two sorts of defects namely, shrinkage and rupture. Consequently, accurate prediction of these phenomena is of particular importance for choosing appropriate path of uploading sheet and making the spherical shape. The widely used spherical products in industry, in particular, gas and petrochemical sectors are rupture discs. These discs are close to spherical shape and play a protective role for high pressure industrial equipment. In case of high pressure in the system, the discs are ruptured and preventing any further harm to the system.

Rupture usually occurs due to the necking caused by local instability under high tensile stresses in the forming process by hard tools. Hydroforming is a process of forming materials in which instead of utilizing hard tools (punch, die, insert, etc.), the fluid pressure (liquid or gas) is employed to yield plastic deformation in a specimen such as sheet or tube. This method has an advantage of one-step process and widely used in the industrial world.

Yossifon and Tirosh in 1985-88, carried out simple analysis on the hydroforming process of aluminum, copper, steel and stainless steel cups [1-2]. Lo et al., continued their researches with a hemispherical shaped punch in 1993 [3]. Hsu and Hsieh in 1996, experimentally investigated the results of this theory and found a good agreement between the theory and the experiment [4]. They also investigated the upper bound pressure for hemispherical shaped punch, like that of Yossifon and Tirosh done for cylindrical shaped punch [1-2].

Lei et al. [5] in 2001, carried out some works on hydroforming process with finite element simulation, in which the process of sheet metal forming was considered. Zampaloni in 2003, studied aluminum sheet hydroforming process both numerically and experimentally [6]. Further in 2005, Abedrabbo reviewed the wrinkling of 6000 series aluminum alloys in sheet hydroforming with a spherical shaped punch both numerically and experimentally [7].

Wu et al., and Khandeparkar and Liewald obtained shrinkage and rupture diagrams for stepped punch with finite element simulations and experimental tests [8], [9]. Thiruvarudchelvan and Tan presented both theoretical and empirical analyses for deep-drawing with hydraulic pressure [10]. Brabie and Ene used neural networks to optimize the hemispherical punch in the forming process and reduced the spring back [11]. Finally, Li and He employed the Hill criterion to accurately describe the mechanical properties of aluminum alloys used in sheet forming and showed that this measure has good ability to express the behavior of anisotropic materials [12]. In this paper, in order to obtain more accurate analytical results, the Hill criterion is used to analyze the rupture phenomena in sheet hydroforming process by hemispherical punch.

2 DIVISION OF WORK PIECE ZONES

To review the hydroforming process of hemispherical punch, the work piece is divided into three zones in which the stresses and the strains are continuous. The division of regions shown in Figure 1, are defined as follows:

1-The region in which, work piece is in contact with the die (Zone I).
2-The region in which, work piece is without support (Zone II).
3-The region in which, work piece is in contact with the punch surface (Zone III).

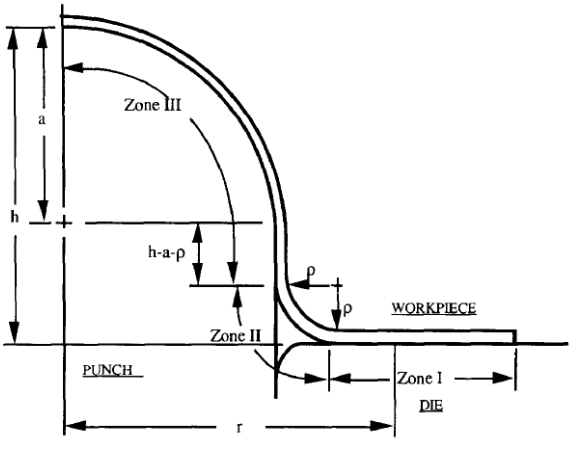

Fig. 1 Three zones of the sheet regions

2.1. Assumptions

Some simplifying assumptions are used to analyze the process as follows:

1- The punch, the die and the clamp are rigid and this is acceptable for plastic deformation and forming process.
2- The thickness of work piece is constant during the process.

3- Due to the fluid pressure and friction in Zone III, the part of the work piece in contact with the punch is assumed to be rigid.
4- In the Zone I, where the work piece is in contact with the die, the friction force is assumed as follows:

$$f = f(p_1) \tag{1}$$

Where p_1 is the clamp force.

5- The resistance against the sheet deformation caused by effective stress, effective strain and material constant is characterized by the power law plasticity:

$$\bar{\sigma} = \sigma_0(\bar{\varepsilon})^n \qquad \bar{\varepsilon} \geq 0.002 \tag{2}$$

Where $\bar{\varepsilon}$ is the effective strain, $\bar{\sigma}$ is the effective stress, n is the strain-hardening exponent and σ_0 is the material constant.

6-The Hill criterion is used to analyze the problem [13]:

$$R(\sigma_Y - \sigma_z)^2 + P(\sigma_z - \sigma_x)^2 + PR(\sigma_x - \sigma_y)^2 = P(R+1)\bar{\sigma}^2 \tag{3}$$

Where, P and R are the sheet anisotropic coefficients respectively along y and x axis.

7-The plane stress and two dimensional isotropic conditions are used in the process:

$$P = R \ , \qquad \sigma_z = 0 \tag{4}$$

8-The plastic flow rule is used to solve the problem:

$$d\varepsilon_{ij} = d\lambda \frac{\partial f(\sigma_{ij})}{\partial \sigma_{ij}} \tag{5}$$

8-The equilibrium equation for an element in polar coordinates with axial symmetry is as follows:

$$\frac{d}{dr}(t\sigma_r) + \frac{t}{r}(\sigma_r - \sigma_\theta) + f(p_1) = 0 \tag{6}$$

2.2. Stress Distribution

Based on the partitioning assigned in the sheet, as well as equation (6) and assumption of constant thickness for Zone I, the following relation will be obtained:

$$\frac{d}{dr}(\sigma_r) + \frac{1}{r}(\sigma_r - \sigma_\theta) + \frac{f(p_1)}{t} = 0 \tag{7}$$

Where, t is the sheet thickness. On the other hand, the following equation exists:

$$\varepsilon_r + \varepsilon_\theta + \varepsilon_z = 0 \qquad \rightarrow \qquad \varepsilon_r = -\varepsilon_\theta \tag{8}$$

According to Hill criterion:

$$f = \varepsilon_r^2 + \varepsilon_\theta^2 + R(\sigma_r - \sigma_\theta)^2 = (R+1)\bar{\sigma}^2 \tag{9}$$

Using equation (5), it would be:

$$\frac{\varepsilon_r}{\frac{\partial f}{\partial \sigma_r}} = \frac{\varepsilon_\theta}{\frac{\partial f}{\partial \sigma_\theta}} = \frac{\bar{\varepsilon}}{\frac{\partial f}{\partial \bar{\sigma}}} \tag{10}$$

Replacement and simplification of above relation would lead to:

$$\sigma_r = -\sigma_\theta \tag{11}$$

Replacing equation (11) into equation (9) would lead to:

$$\bar{\sigma} = \left(\frac{4\sigma_r^2}{R_e}\right)^{1/2} \tag{12}$$

Where R_e is defined as follows:

$$R_e = \frac{2(1+R)}{1+2R} \tag{13}$$

According to the geometry and problem conditions for hemispherical shaped punch, the radial stress will be always greater than zero and the tangential stress will be negative; also by using equations (2), (7), (11) and (12), the following equation would be obtained:

$$\frac{d}{dr}(\sigma_r) + \frac{1}{r}(\sigma_0(\bar{\varepsilon})^n \sqrt{R_e}) + \frac{f(p_1)}{t} = 0 \tag{14}$$

The rate of effective strain for the condition of plane strain will be as follows:

$$\dot{\bar{\varepsilon}} = \frac{1+R}{\sqrt{1+2R}}\left[(\dot{\varepsilon}_r)^2 + \frac{2R}{1+R}\dot{\varepsilon}_r\dot{\varepsilon}_\theta + (\dot{\varepsilon}_\theta)^2\right]^{1/2} \tag{15}$$

According to the equation (8) and integrating the equation (15), the effective strain will be as follows:

$$\bar{\varepsilon} = \sqrt{R_e}\,\varepsilon_r \tag{16}$$

Where

$$\varepsilon_r = -\int_{r_0}^{r} \frac{dr}{r} = \ln \frac{r_0}{r} \tag{17}$$

The maximum stroke of the punch in this analysis is confined to the limit of hemisphere shape of sheet metal. According to the constant area of the sheet and using the relations of Hsu et al., [4], the following inequity will be obtained:

$$(a+\rho)\cos\alpha \le r \le b \tag{18}$$

In which, α is the punch radius, ρ is the sheet curvature in Zone II and b is radius of the circular sheet as shown in Fig. 1. The value of r_0 is:

$$r_0 = G = a\{(\frac{r}{a})^2 - (1+\frac{\rho}{a})^2\cos^2\alpha + 2(1-\sin\alpha)[1-(\frac{\rho}{a})^2] + 2(\frac{\rho}{a})\times(1+\frac{\rho}{a})(\frac{1}{2}\pi-\alpha)\cos\alpha\}^{1/2} \tag{19}$$

According to the geometry of Fig. 1 :

$$\alpha = \sin^{-1}(\frac{(a+\rho-h)}{(a+\rho)}) \tag{20}$$

Where, h is the punch stroke. Using equations (14) and (16) will lead to:

$$\frac{d}{dr}(\sigma_r) + \frac{1}{r}(\sigma_0(\varepsilon_r)^n \times (R_e)^{\frac{n+1}{2}}) + \frac{f(p_1)}{t} = 0 \tag{21}$$

Integrating equation (20) will lead to the radial stress in Zone I:

$$\sigma_r^{(I)}(r) = \int_r^b \frac{f(p_1)}{t}dr + \int_r^b \frac{(\sigma_0(\varepsilon_r^I)^n R_e^{\frac{n+1}{2}}}{r}dr \tag{22}$$

Based on the fact that the radial stress is continuous and neglecting the friction and bending stress, the radial stress in Zone II will be as follows:

$$\sigma_r^{(II)}(r) = \sigma_r^{(I)}(r=(a+\rho)\cos\alpha) + \int_r^{(a+\rho)\cos\alpha} \frac{(\sigma_0(\varepsilon_r^{II})^n R_e^{\frac{n+1}{2}}}{r}dr \tag{23}$$

With equation (17) in Zone II (where the work piece is without support), the following inequity will be obtained:

$$a \le r \le (a+\rho)\cos\alpha \tag{24}$$

Likewise,

$$r_0 = f = \sqrt{2}a\times(1-\sin\alpha+(\frac{\rho}{a})[(1+\frac{\rho}{a})\times(\frac{1}{2}\pi-\alpha-\beta)\times\cos\alpha]+(\frac{\rho}{a})(\sin\alpha-\cos\beta))^{1/2} \tag{25}$$

According to Fig. 1:

$$\beta = \sin^{-1}(\frac{(a+\rho)\cos\alpha - r}{\rho}) \tag{26}$$

Hence, the radial stress in Zone II will be:

$$\sigma_r^{(II)}(r) = \int_r^{(a+\rho)\cos\alpha} \frac{\sigma_0(\varepsilon_r^{II})R_E^{\frac{n+1}{2}}}{r}dr + \int_{(a+\rho)\cos\alpha}^b \frac{f(p_1)}{t}dr + \int_{(a+\rho)\cos\alpha}^b \frac{\sigma_0(\varepsilon_r^I)^n R_E^{\frac{n+1}{2}}}{r}dr \tag{27}$$

3 INVESTIGATING THE RUPTURE

Moore and Wallace [14] predicted the instability of anisotropic materials under the condition of biaxial plane strain as follows:

$$\frac{d\bar{\sigma}}{d\bar{\varepsilon}} = \frac{\bar{\sigma}}{z} \tag{28}$$

Where,

$$z = \frac{(1+R)}{\sqrt{1+2R}} \tag{29}$$

Combining Eqs. (2) and (28) will lead to the effective critical strain:

$$\bar{\varepsilon}_r = nz \tag{30}$$

Using Eqs. (2), (16), (29), and (30), the equation of critical radial stress for the sheet rupture will be obtained:

$$\varepsilon_r^{cr} = \frac{\sigma_0 n^n}{2}(\frac{1+R}{\sqrt{1+2R}})^n \sqrt{R_e} \tag{31}$$

In the common point of Zones II and III, high tendency of the rupture is found. Therefore, according to Fig. 1, the critical radius will be as follows:

$$r = a\cos\alpha \tag{32}$$

Using Eqs. (27), (31), (17) and (32), with the friction obtained from Eq. (33) and further simplifications, Eq. (34) will be obtained:

$$f(p_1)=2\mu p_1 \tag{33}$$

$$\frac{n^n}{2}\left(\frac{1+R}{\sqrt{1+2R}}\right)^n\sqrt{R_e}=\int_{a\cos\alpha}^{(a+\rho)\cos\alpha}\frac{(\ln\frac{f}{r})^n R_e^{\frac{n+1}{2}}}{r}+\int_{(a+\rho)\cos\alpha}^{b}\frac{(\ln\frac{G}{r})R_e^{\frac{n+1}{2}}}{r}dr+\frac{2\mu p_1}{\sigma_0 t}(b-(a+\rho)\cos\alpha) \tag{34}$$

Where, μ is the coefficient of friction between the sheet-clamp and the sheet-punch. In Fig. 1, if the bending stress is neglected and the radial stress is calculated, Zone II may be shown as in Fig. 2:

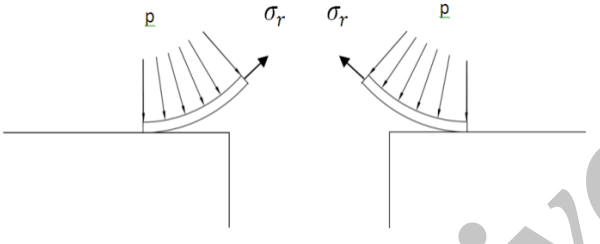

Fig. 2 The Zone between two sheets under the fluid pressure

From force equilibrium, it is obtained :

$$\sigma_r^{II}(r_\alpha)=\frac{p\rho(2a+\rho)}{2at} \tag{35}$$

$$r_\alpha=a\cos\alpha \tag{36}$$

Also, by equating Eqs. (35) and (27), the following equation is obtained:

$$\frac{\sigma_0 n^n}{2}\left(\frac{1+R}{\sqrt{1+2R}}\right)\sqrt{R_e}=\frac{p\rho(2a+\rho)}{2at} \tag{37}$$

In order to obtain the critical pressure with the new assumption of Hill criterion, solution of equations (34) and (37) are needed using common methods in numerical calculations.

4 NUMERICAL CALCULATIONS

For solving integrals in equation (34), Gauss-Legendre eight point method and for finding the roots, Newton-Raphson method could be used. By integrating it in the range [*a*, *b*] we have:

$$\int_a^b f(t)dt\approx\frac{b-a}{2}\sum_{j=1}^{n}w_j f\left(\frac{a+b}{2}+x_j\frac{b-a}{2}\right) \tag{38}$$

Where, w_js are the integrating weights for the Gauss-Legendre eight point method. The Newton-Raphson method is as follows:

$$P_{n+1}=P_n-\frac{f(P_n)}{f'(P_n)} \tag{39}$$

For derivative of the function, the following formula is used:

$$f'(x)\approx\frac{f(x+\varepsilon)-f(x)}{\varepsilon} \tag{40}$$

In which, ε is a number with magnitude of 10^{-6}. Using Table 1, data for the material conditions and experimental results in ref. [6], could lead to solving the equations (34) and (37).

Table 1 Problem conditions

t	1 mm	*n*	0.0476
a	50.8 mm	*R*	0.89
b	88.9 mm	*μ*	0.13
p_1	482 MPa	σ_0	202.4MPa

The calculated results are shown in Fig. 3, which is compared with the Tresca based results.

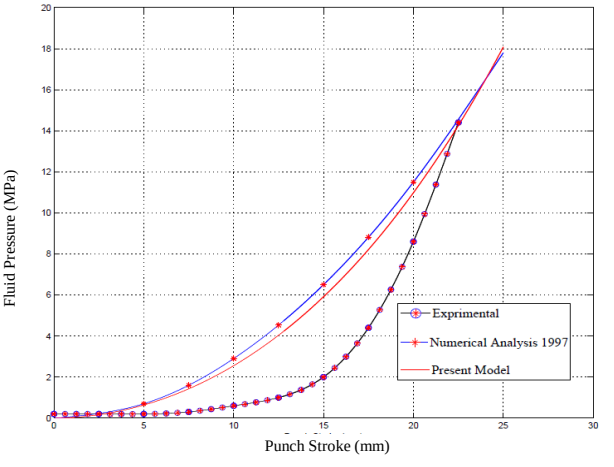

Fig. 3 Upper bound of fluid pressure in hydroforming process

5 THE RESULTS AND DISCUSSION

In the hydroforming and deep drawing processes, due to the environmental forces, the sheet edges in zone I are prone to shrinkage and wrinkles; whilst in the common area of zones II and III, the sheet is in stretching mode. Thus, the sheet forming is enclosed between the two areas. If by progressing the punch, back pressure of the sheet is reduced, the forming path exceeds the lower limit and the earring and wrinkling defects take place. Inversely, if by progressing the punch, back pressure of the sheet is increased, the forming path exceeds the upper limit and the rupture phenomenon occurs. Therefore, as the distance between the upper and lower limits is getting wider, the more chance of desirable for plate forming.

Material properties and geometry have great effects on the fluid upper bound pressure. In the following, with changing the geometric and material parameters, the variation of upper limit or rupture limit will be studied based on the Hill criterion. Among geometric parameters, the thickness has an important effect on the upper bound pressure. Reducing the work piece thickness will decrease the pressure sustain; while increasing the thickness will increase pressure sustain in the work piece, as shown in Fig. 4.

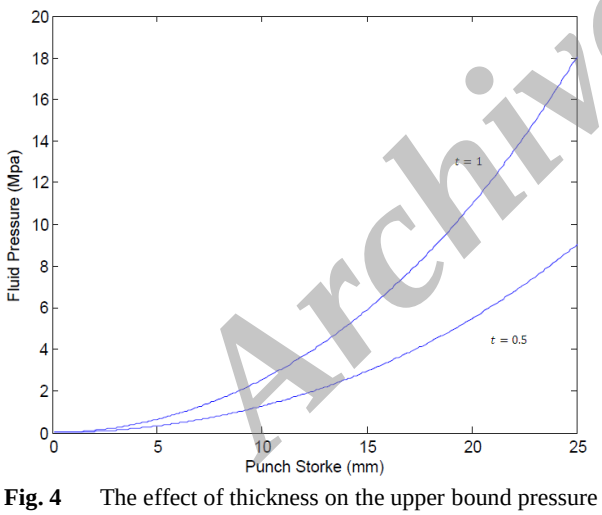

Fig. 4 The effect of thickness on the upper bound pressure

Increasing friction coefficient will raise the friction force and will reduce the upper bound pressure, as shown in Fig. 5. Decreasing the ratio of sheet radius to of punch will increase the upper bound pressure of fluid. Since the region of under clamp decreases, in result the contact surface between clamp and sheet, as well as sheet and die will decrease. This will lead to further reduction of friction force and increasing the upper bound pressure as shown in Fig. 6. Furthermore, increasing the anisotropic coefficient will raise the upper bound pressure as in Fig. 7.

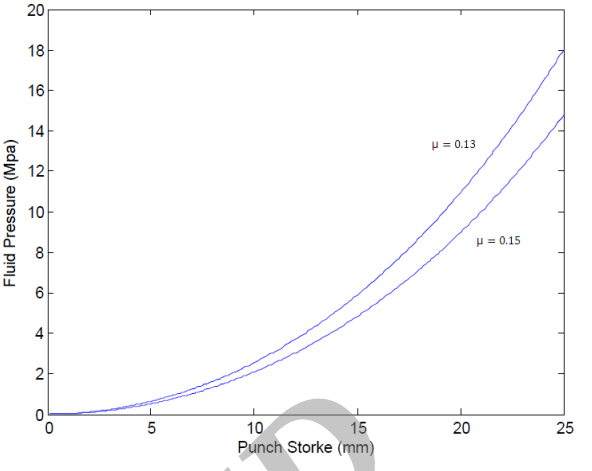

Fig. 5 The effect of friction coefficient on the upper bound pressure

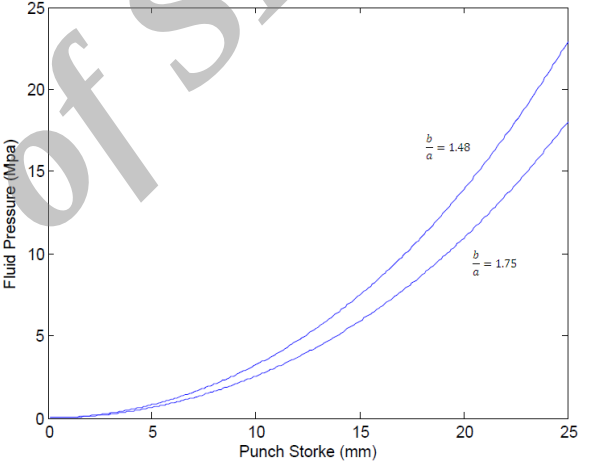

Fig. 6 The effect of the ratio of sheet radius to of punch on the upper bound pressure

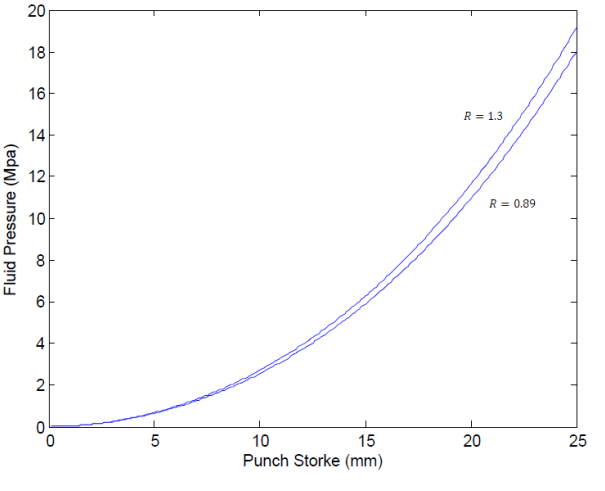

Fig. 7 The effect of anisotropic coefficient on the upper bound pressure

In addition, increasing the work hardening parameter will lead to rising the rupture point as shown in Fig. 8.

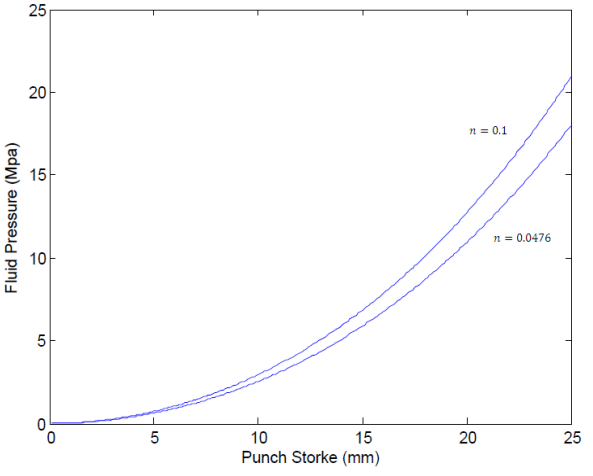

Fig. 8 The effect of work hardening parameter on the upper bound pressure

6 CONCLUSION

According to Fig. 3, the rupture limit obtained from the Hill and Tresca criteria are close together, and its intersection with the experimental curve shows that the rupture depth is nearly identical. Due to compressive circumferential and tensile stresses created in the sheet and in regard to Fig. 9, it can be seen that in the fourth zone, the Hill criterion with Tresca criterion are practically the same.

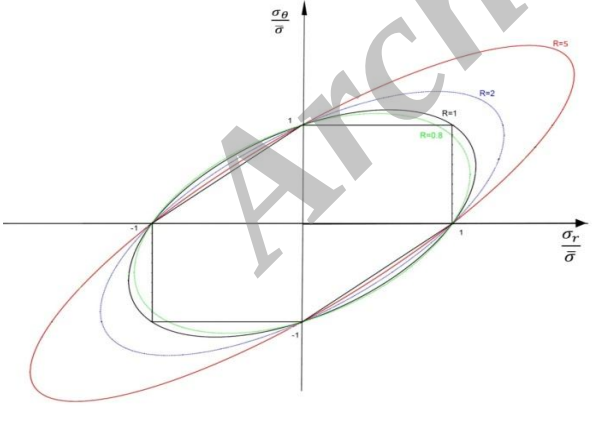

Fig. 9 The effect of work hardening on the upper bound pressure

Investigating the effects of geometry and material properties on the rupture limit, it can be observed that the effect of geometric parameter is much greater than that of material properties. Increasing the thickness, work hardening and anisotropy property, cause the increase of upper bound pressure, which is desirable for the sheet forming. Furthermore, increase in the ratio of sheet radius to punch radius as well as friction augmentation cause the decrease of upper bound pressure which is undesirable.

REFERENCES

[1] Yossifon, S. Tirosh, J., "Rupture instability in hydro-forming deep-drawing process", Int. Journal Mech. Science, Vol. 27, June 1985, pp. 559- 570.

[2] Yossifon, S. Tirosh, J., "On the permissible fluid-pressure path in hydro-forming deep drawing processes-analysis of failure and experiments", Journal Eng. Ind., Vol. 110, May 1988, pp. 146-152.

[3] Lo, S. W., Hsu, T. C., and Wilson, W. R. D., "An analysis of the hemispherical punch hydro-forming process", Journal of Materials Processing Technology, Vol. 37, 1993, pp. 225-239.

[4] Hsu, Tze-chi Hsieh, Shian-Jiann, "Theoretical and experimental analysis of failure for the hemisphere punch hydro-forming processes", Int. Journal Manuf. Science and Engineering, Vol. 3, 118/434-438, 1996.

[5] Lei, L. P., Kang, B. S. and Kang, S. J., "Prediction of forming limit in hydro-forming process using the finite element method and a ductile fracture criterion", Journal of Materials Processing Technology, Vol. 113, 2001, pp. 673-679.

[6] Zampaloni, M., Abedrabbo, N. and Pourboghrat, F., "Experimental and numerical study of stamp hydro-forming of sheet metals", Int. Journal Mech. Sciece, Vol. 45, 2003, pp. 1815-1848.

[7] Abedrabbo, N., Zampaloni, M. and Pourboghrat, F., "Wrinkling control in aluminum sheet hydro-forming", International Journal of Mechanical Sciences, Vol. 47, 2005, pp. 333-358.

[8] Wu, J., Balendra, R., and Qin, Y., "A study on the forming limits of the hydro mechanical deep drawing of components with stepped geometries", Journal of Materials Processing Technology, Vol. 145, 2004, pp. 242-246.

[9] Khandeparkar, T., Liewald, M., "Hydro mechanical deep drawing of cups with stepped geometries", Journal of Materials Processing Technology, Vol. 202, 2008, pp. 246-254.

[10] Thiruvarudchelvan, S., Tan, M. J., "A note on fluid pressure-assisted deep drawing processes", Journal of Materials Processing Technology, Vol. 172, 2008, pp. 174-181.

[11] Brabie, G., Ene, F., "Application of the neural network method in optimization of the drawing process of hemispherical parts made from metal sheets", Journal of Archives of Civil and Mechanical Engineering, Vol. 6, No. 2, 2006, pp. 87-92.

[12] Xiao-qiang Li, De-hua He, "Identification of material parameters from punch stretch test", Journal of Transactions of Nonferrous Metals Society of China, 2013, Vol. 23, No. 5, May 2013, pp. 1435-1441.

[13] Hill, R., "The mathematical theory of plasticity", Oxford: Clarendon Press, 1950.

[14] Moore, G. G., Wallace, J. F., "The effect of anisotropy on instability in steel-metal forming", Journal Inst. of Metals, Vol. 93, 1965, pp. 33-38, 1965.